Supporting Information

Isomeric Identification of the Nitroindole Chromophore in Indole + NO_3 Organic Aerosol

*Avery B. Dalton, Lisa M. Wingen, and Sergey A. Nizkorodov**

Department of Chemistry, University of California, Irvine, Irvine, CA 92697

Contents

UHPLC-HESI-HRMS Methods

Sample volumes of 10 µL were injected onto a an ACQUITY HSS T3 C18 column (Waters, 2.1 ID, 150 mm length, 1.8 µm particle size) equipped with an ACQUITY UPLC HSS PFP VanGuard pre-column (2.1 mm, 5 mm, 1.8 µm), both maintained at 30 °C. The mobile phase flowed at 300 µL min^{-1} and was composed of A, H_2O (Fisher Chemical, Optima, LCMS grade) containing 0.1% formic acid (Fisher Chemical, Optima, LCMS grade), and B, acetonitrile (Fisher Chemical, Optima, LCMS grade) containing 0.1% formic acid. A gradient elution was used with 5% B held for 3 minutes, a linear increase to 95% B over a 11-min period, 95% B held for 2 min, and returned to 5% B and held for 6 min. The heated electrospray ionization source was used with a spray voltage set in positive ion mode to 4.0 kV, a capillary temperature maintained at 325°C, a sheath gas flow rate of 35 (arbitrary units; a.u.), an auxiliary gas flow rate of 10 (a.u.), a sweep gas flow rate of 8 (a.u.), an S-lens RF level at 30 (a.u.), and an auxiliary gas heater temperature of 300°C. Settings used in negative ion mode were the same except for a sheath gas flow rate of 50, a sweep gas flow rate of 1, a capillary temperature of 320°C, and a spray voltage of 2.5 kV.

UV/Vis Results

Table S1. Comparison of peak positions from UV/vis absorption spectra in 2-propanol, recorded with a spectrophotometer, and in acetonitrile/water (ACN/H_2O), recorded with PDA.

Isomer	**λ_{max} in 2-propanol**	**λ_{max} in ACN/H_2O**
Indole + NO_3 SOA	-	354 nm
3-nitroindole	349 nm	354 nm
4-nitroindole	377 nm	384 nm
5-nitroindole	322 nm	327 nm
6-nitroindole	324 nm (major) 364 nm (minor)	332 nm (major)
7-nitroindole	365 nm	369 nm

The absorption spectra had slight differences between the measurements taken in 2-propanol, with the spectra recorded in the UHPLC mobile phase (ACN and H_2O) typically exhibiting a redshift in the visible region compared to spectra recorded in 2-propanol. This could be indicative that the lower lying excited singlet states are more polar compared to their ground states. The effects of changing solvent are less obvious for higher excited states since the resolution for peaks below 300 nm is inferior for the PDA in the UHPLC system.

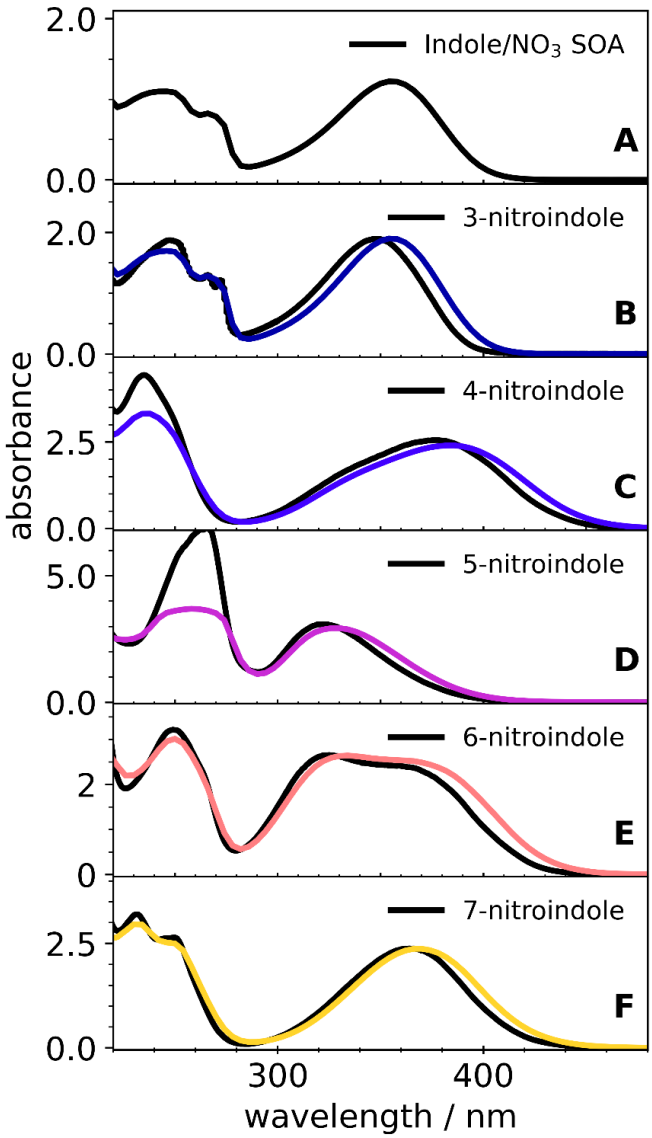

Figure S1. UV/Vis absorption spectra for each nitroindole isomer evaluated in this work. Colored traces were measured with the PDA using the water + acetonitrile eluent as solvent, and the black traces were recorded with the bench-top UV/Vis using 2-propanol as solvent. Small spectral shifts are observed relative to the peak wavelengths in the UHPLC-PDA measurements, likely due to the different solvent (water-acetonitrile mixture at pH = 3).

Chromatographic Results

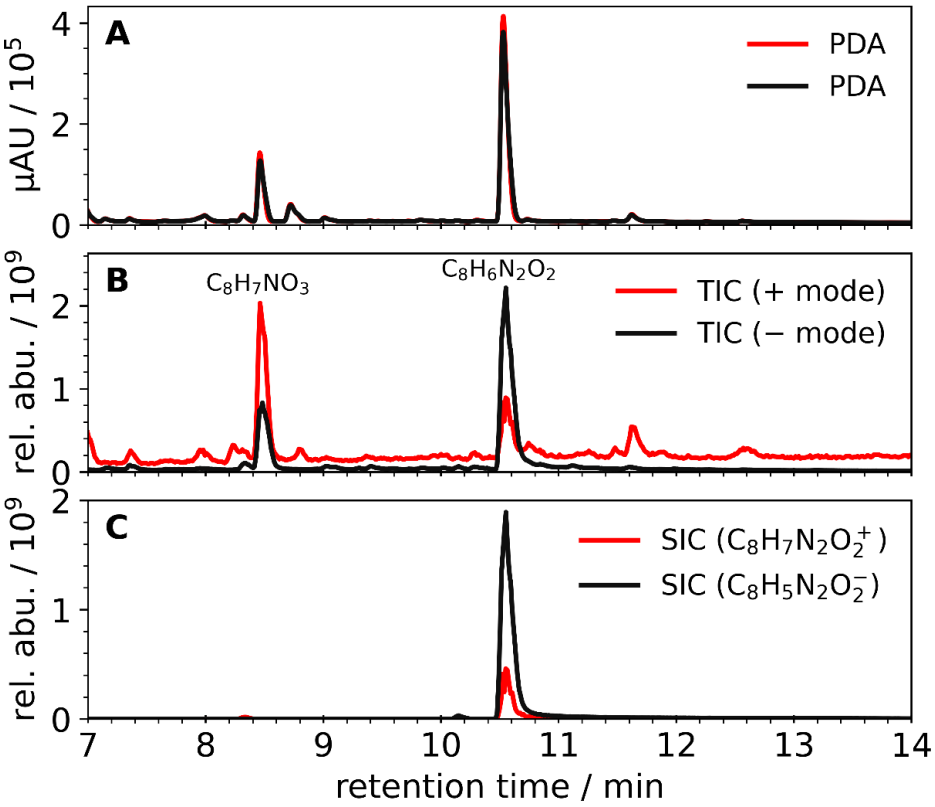

Figure S2. PDA (panel A), total ion current (TIC, panel B), and selected ion current (SIC, panel C) chromatograms for indole + NO_3 SOA, run in heated electrospray ionization positive mode (red) and negative mode (black). Panel C shows that one isomer of nitroindole is preferentially produced.

An Unfavorable Alternative: NO_3 Attachment

Given the previous studies which showed that attachment at P2 was favored in indole for other radicals, the analogous reaction was tested here for NO_3 with DFT. We also attempted to do these calculations at MP2 level but limitations in computational resources made it difficult to compute frequencies for many of the intermediates at the MP2 level. Namely, the finite difference calculations required to compute the frequencies, which inherently take a long time, were often interrupted by issues with the SCF calculations. In some cases, warnings regarding linear dependencies in the AO basis sets appeared, which we attempted to alleviate with tighter screening thresholds and even trying less diffuse basis sets. Given these difficulties, and the appearance of two large transition state energy barriers predicted by DFT in Fig. S3, we elected to pause on the MP2 calculations for this pathway and rely on the DFT results.

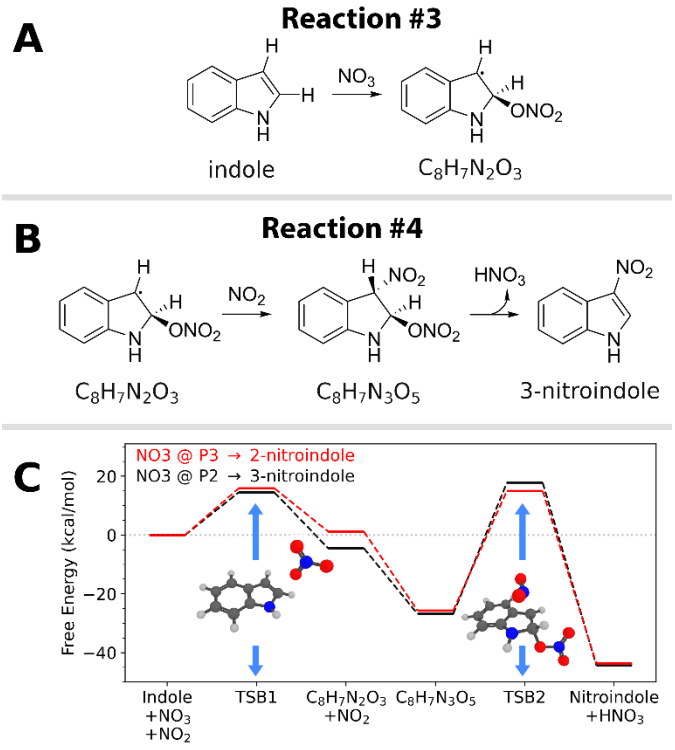

Figure S3. Hypothetical reaction mechanisms for a reaction pathway in which the NO_3 attaches directly to pyrrole component of indole. This pathway is comprised of A) Reaction #3 and B) Reaction #4, which represent the attachment of NO_3 and NO_2 respectively. In C) is a free energy diagram (PBE0/6-311++G(d,p)) showing the Gibbs free energies of each structure with respect to all three reactants (indole, NO_3, and NO_2).

ToF-AMS Analysis

Particles were sampled with the ToF-AMS (Aerodyne) at ~0.08 LPM, vaporized at 600°C, and ionized by electron impact ionization (70 eV). Spectra were collected in V mode from *m/z* 10-440 with a mass resolving power of m/Δm ~2100. A particle filter was used to account for small amounts of gas phase CO_2 in the Teflon chamber.

Analysis was performed using software packages SQUIRREL v1.66E and PIKA v1.26E with Igor Pro (WaveMetrics, v.8.04) with default values for relative ionization efficiencies and for the fragmentation table, except where noted below.

The AMS unit-mass and high resolution (HR) fragmentation tables were modified for the 3-nitroindole standard only, such that the CO^+ intensity was not set equal to the CO_2^+ intensity, and CO^+ fitting was omitted altogether to avoid interference from the large N_2^+ signal at *m/z* 28. This is because, although a particle filter was used to 'zero' small amounts of gas phase CO_2 present in the chamber, a CO_2^+ signal was still detected at *m/z* 43.99 for the 3-nitroindole standard (Figure 3a,b). CO_2^+ fragments are not expected for this compound since there are no carboxylic acid functional groups. A plot of the CO_2^+ fragment as a function of fragments assigned to 3-nitroindole, e.g., $C_7H_5^+$ at *m/z* 89 and $C_8H_6NO^+$ at *m/z* 132 (see Table 1, main text) shows that the CO_2^+ signal increases with mass concentration of 3-nitroindole (Figure S4, blue symbols) and suggests that this signal may arise from decomposition reactions on the vaporizer. A similar observation was reported in a previous study of the decomposition of NH_4NO_3, in which high levels of NO and NO_2 that form during vaporization were observed to react with carbon-containing matter present on the vaporizer surface, leading to CO and CO_2 (and their ions).[1] CO^+ fragments are also not expected for 3-nitroindole, but are difficult to quantify due to the large N_2^+ signal at *m/z* 28 from gas phase N_2. Examination of AMS particle time-of-flight data for *m/z* 28 showed that CO^+ did not have a signal in the size range of the particles. Thus, CO^+ was omitted. No changes were made for the SOA mass spectra (i.e., the default HR fragmentation tables were used) since there are multifunctional compounds present in indole SOA, including the likelihood of carboxylic acids. The default unit-mass and HR fragmentation tables assign equal peak heights to the CO^+ and CO_2^+ fragments based on data from multifunctional compounds, where it is generally true that CO^+/CO_2^+ ~1.[2] The expected ratio of CO^+/CO_2^+ is unknown for indole SOA but is assumed to be ~1 here.

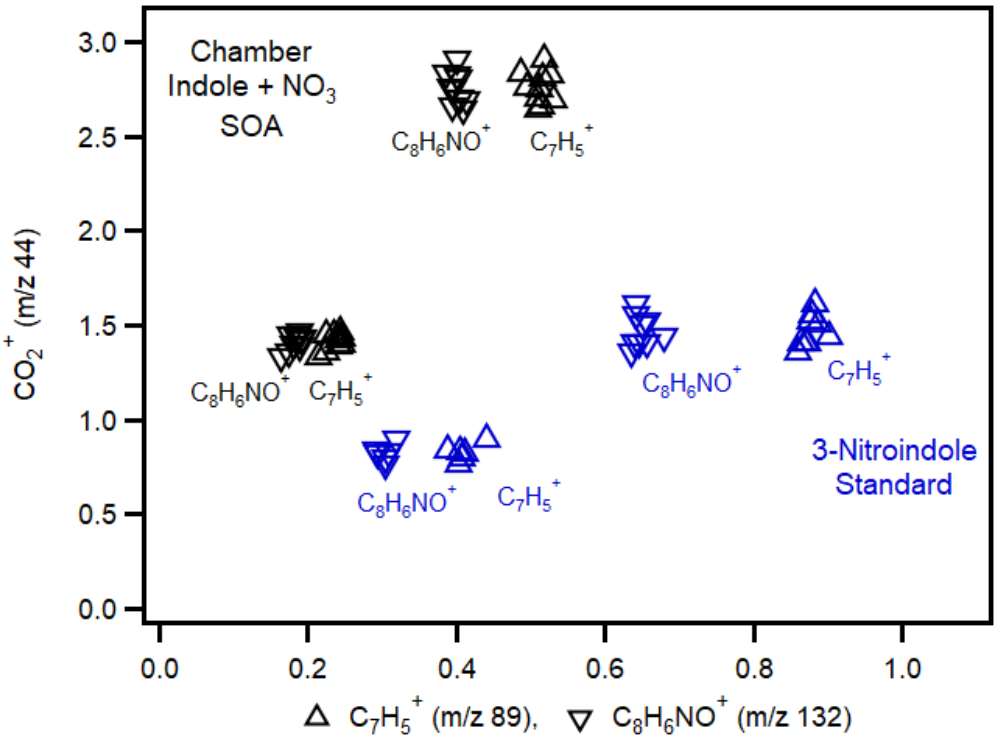

Figure S4. A plot of the CO_2^+ fragment as a function of two typical fragments of 3-nitroindole shows that the CO_2^+ signal increases with mass concentration of 3-nitroindole (blue symbols). Given that 3-nitroindole contains no functional groups that would form CO_2^+, this signal may arise from decomposition reactions on the vaporizer. In contrast, indole SOA components (black symbols) are multifunctional and these CO_2^+ fragments likely arise from carboxylic acid moieties.

The relative ionization efficiency (RIE) of 3-nitroindole in the AMS was determined following a procedure similar to that of Nault et al.[3] Particles of known mobility diameter were introduced to the AMS using an electrostatic classifier (TSI, model 3082) with a long DMA. A CPC (TSI, model 3756) was used to measure the number concentration of 3-nitroindole particles delivered to the AMS. As described above, the 3-nitroindole solution was atomized, dried with two diffusion dryers, and flowed through a carbon denuder to remove remaining solvent. Particles were size-selected at 100 nm and a particle concentration of 150-200 particles cm^{-3} was measured simultaneously during AMS measurements of mass spectra and PToF size distributions. The low particle concentration provided an undetected level of doubly charged particles. While a larger selected diameter would be better suited to minimize doubly charged particles, they were not able to be selected with the particle sizes generated from atomization. The RIE of 3-nitroindole was

calculated by comparing the mass concentration measured by the AMS using an RIE of 1.0 to the mass concentration calculated from the CPC-measured number concentration, the selected diameter, and the density. An approximate density of 1.4 ± 0.1 g cm^{-3} is reported as a predicted value (ChemSpider, CSID:9259328, accessed May 2024). This density is consistent with AMS particle time-of-flight measurements, assuming spherical particles, in which size-selected 100 nm mobility diameter particles resulted in an average vacuum aerodynamic diameter of 133 ± 7 (1s) nm.[4] We report an RIE for 3-nitroindole of $RIE_{3\text{-}NI}$ = 2.6 ± 0.6. This range of 2.0 – 3.2 for the RIE includes uncertainties in the density as well as the mass concentration reported by the AMS. $RIE_{3\text{-}NI}$ is higher than the default ionization efficiency of 1.4 often used for organic aerosol, thus the AMS is more sensitive to nitroindole than other organics. The AMS reference mass spectra generated in this study have been made available in the AMS database https://cires1.colorado.edu/jimenez-group/AMSsd/.[5,6]

Recently, Nault et al. reported that organic aerosol (OA) standards whose AMS spectra have a high fraction of intensity below *m/z* 50 ($f_{\Sigma m/z50}$ > 64%) yielded an average RIE_{OA} of 1.23 ± 0.62, leading to their recommendation of using the default value of RIE_{OA} = 1.4.[3] They showed in contrast that organic compounds with AMS spectra containing a large number of fragments above *m/z* 50 tend to have RIE > 1.4. Interestingly, the AMS spectrum of 3-nitroindole has a value of $f_{\Sigma m/z50}$ of 33% (only 33% of peak intensity is below *m/z* 50) and several prominent fragments are above *m/z* 50. Thus, an $RIE_{3\text{-}NI}$ = 2.6 ± 0.6 is consistent with the trend reported by Nault et al.

References

(1) Pieber, S. M.; El Haddad, I.; Slowik, J. G.; Canagaratna, M. R.; Jayne, J. T.; Platt, S. M.; Bozzetti, C.; Daellenbach, K. R.; Fröhlich, R.; Vlachou, A.; Klein, F.; Dommen, J.; Miljevic, B.; Jiménez, J. L.; Worsnop, D. R.; Baltensperger, U.; Prévôt, A. S. H. Inorganic Salt Interference on CO_2^+ in Aerodyne AMS and ACSM Organic Aerosol Composition Studies. *Environ. Sci. Technol.* **2016**, *50* (19), 10494–10503. https://doi.org/10.1021/acs.est.6b01035.

(2) Canagaratna, M. R.; Jimenez, J. L.; Kroll, J. H.; Chen, Q.; Kessler, S. H.; Massoli, P.; Hildebrandt Ruiz, L.; Fortner, E.; Williams, L. R.; Wilson, K. R.; Surratt, J. D.; Donahue, N. M.; Jayne, J. T.; Worsnop, D. R. Elemental Ratio Measurements of Organic Compounds Using Aerosol Mass Spectrometry: Characterization, Improved Calibration, and Implications. *Atmospheric Chemistry and Physics* **2015**, *15* (1), 253–272. https://doi.org/10.5194/acp-15-253-2015.

(3) Nault, B. A.; Croteau, P.; Jayne, J.; Williams, A.; Williams, L.; Worsnop, D.; Katz, E. F.; DeCarlo, P. F.; Canagaratna, M. Laboratory Evaluation of Organic Aerosol Relative Ionization Efficiencies in the Aerodyne Aerosol Mass Spectrometer and Aerosol Chemical Speciation Monitor. *Aerosol Science and Technology* **2023**, *57* (10), 981–997. https://doi.org/10.1080/02786826.2023.2223249.

(4) DeCarlo, P. F.; Slowik, J. G.; Worsnop, D. R.; Davidovits, P.; Jimenez, J. L. Particle Morphology and Density Characterization by Combined Mobility and Aerodynamic Diameter Measurements. Part 1: Theory. *Aerosol Science and Technology* **2004**, *38* (12), 1185–1205. https://doi.org/10.1080/027868290903907.

(5) Ulbrich, I. M., Canagaratna, M. R., Zhang, Q., Worsnop, D. R., and Jimenez, J. L. Interpretation of organic components from Positive Matrix Factorization of aerosol mass spectrometric data, *Atmospheric Chemistry and Physics* **2009**, *9* (9), 2891–2918. https://doi.org/10.5194/acp-9-2891-2009.

(6) Jeon, S., Walker, M. J., Sueper, D. T., Day, D. A., Handschy, A. V., Jimenez, J. L., and Williams, B. J. A searchable database and mass spectral comparison tool for the Aerosol Mass Spectrometer (AMS) and the Aerosol Chemical Speciation Monitor (ACSM), *Atmospheric Measurement Techniques* **2023**, *16* (24), 6075–6095. https://doi.org/10.5194/amt-16-6075-2023.